

Brief Reports

Brief Reports are short papers which report on completed research or are addenda to papers previously published in the Physical Review. A Brief Report may be no longer than 3½ printed pages and must be accompanied by an abstract.

Coulomb effects in the alpha-induced deuteron breakup

M. Bruno, F. Cannata, M. D'Agostino, M. L. Fiandri, and M. Frisoni

*Dipartimento di Fisica dell'Università and Istituto Nazionale di Fisica Nucleare, Sezione di Bologna,
I-40126 Bologna, Italy*

H. Oswald,* P. Niessen, J. Schulte-Uebbing,† and H. Paetz gen. Schieck‡
Institut für Kernphysik, Universität Köln, D-5000 Köln, Federal Republic of Germany

P. Doleschall

Central Research Institute for Physics, H-1525 Budapest, Hungary

M. Lombardi

Istituto Nazionale di Fisica Nucleare, Laboratori Nazionali di Legnaro, Legnaro, Italy

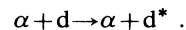
(Received 4 August 1986)

New calculations including an approximate treatment of Coulomb effects in the α -induced deuteron breakup reaction are compared with existing experimental results at $E_d=6$ and 7 MeV and with new measurements at $E_\alpha=11.3$ MeV. The α -p Coulomb potential allows the coupling to the 1S_0 np channel which can give rise to a sharp peak in the $E_{np}=0$ region. We display the relevance of the two-body final state interactions and, in particular, of the isospin forbidden np singlet interaction, both theoretically and experimentally.

The relevance of Coulomb effects in the α -induced deuteron breakup may be tested by measurements at sufficiently low energies.¹⁻³ The experimental data in the region of $E_d=10$ MeV (Ref. 4) and higher energies⁵⁻⁷ are reasonably well reproduced by theoretical calculations, even including polarization quantities. Nevertheless, there are regions where the theoretical predictions differ considerably from experimental data; recently experimental data and calculations including the Coulomb force only as a final state effect showed a discrepancy at low energies.^{3,6} The inadequate treatment of the Coulomb force may be the main reason for this discrepancy. Indeed the effect of the Coulomb interaction is expected to be stronger at low energies.

It is not clear *a priori* if a reliable but still simple approximation for treating Coulomb effects can be performed.⁸ The full theoretical treatment is still in an exploratory stage because it presents both mathematical and practical difficulties. Phenomenological suggestions are thus needed in order to understand the relevance and some qualitative features of these effects. In this spirit we have performed new measurements at $E_\alpha=11.3$ MeV which complement previous measurements at the same energy.² The kinematical configurations have been chosen in order to allow for d^* production at various angles ϑ_{d^*} in the

center of mass for the two-body reaction:



The experimental apparatus has been extensively described elsewhere.² We used the doubly ionized ^4He beam of the 7 MV Van de Graaff accelerator of the Laboratori Nazionali di Legnaro and thin foils of deuterated polystyrene as targets. The energies of protons and α particles emitted in coincidence were measured by two surface barrier detectors at opposite sides with respect to the beam. An additional detector was used to measure recoil deuterons from elastic scattering. In addition, we present data taken at the Köln FN tandem accelerator. Essentially they are part of an excitation function at a fixed c.m. angle of the emitted protons, but with no preference for d^* production.^{6,7} The experiment was performed with vector polarized deuterons to compare also the analyzing power with predictions from Faddeev calculations. Here we discuss only the differential cross sections in the energy region close to the 1^+ level of the intermediate ^6Li , i.e., at 6 and 7 MeV deuteron incident energy. The details of the experiment have been described in Refs. 6, 7, and 9. For both experiments very similar methods of data analysis were used.^{2,9}

Three-dimensional events ($E_p, E_\alpha, \Delta t_{ap}$) were stored on magnetic tape event by event. Δt_{ap} is the difference of the time of flight between α and p and was used to remove unwanted background and for particle identification. After background subtraction the events were projected onto the kinematical curve in order to have a global comparison with theoretical predictions.

The breakup events selected following the procedure described in Refs. 2 and 6 together with the measurement of the recoil deuterons from $\alpha + d$ elastic scattering, assuming the cross section to be known from previous measurements,¹⁴ lead to the determination of absolute cross sections as a function of the arc length, i.e., the length of the kinematical curve. Errors have been estimated adding both statistical and nonstatistical errors in elastic cross sections, solid angle uncertainty, etc. Figure 1 shows the results obtained in four different kinematical configurations at the same α incident energy of 11.3 MeV; Fig. 2 shows the cross sections for deuteron incident energies $E_d = 6$ and 7 MeV.

Two models^{10,11} are used to calculate the effect of the Coulomb interaction on the breakup reaction. In the first ($M1$) the pure Coulomb interaction in the Faddeev calculations is neglected, but in the final expression for the breakup T matrix the α -proton two-body t matrix was modified in order to reproduce the experimental αp phase shifts.^{12,13} In the second model ($M2$) one imitates¹¹ an intermediate range repulsion ($4.5 \text{ fm} \leq R \leq 10 \text{ fm}$) of ~ 0.5 MeV height in the α -proton interaction. The two models are rather crude, since a single-term separable approximation has been used for the αn and αp interaction; they can only be relevant as an indication for the dynamics revealed by the experimental data. The $M2$ model has been found to be qualitatively more satisfactory than the $M1$.¹¹ So here we will present the model calculation $M2$ with

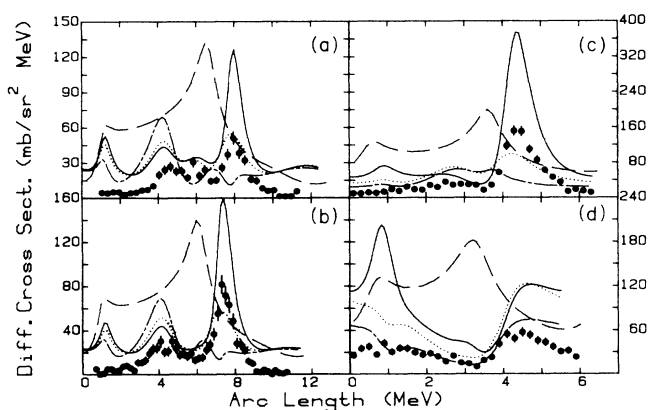


FIG. 1. Experimental results of the reaction $\alpha + d \rightarrow \alpha + p + n$ at $E_\alpha = 11.3$ MeV. Kinematical configurations: (a) $\vartheta_\alpha = 12.7^\circ$, $\vartheta_p = 13.5^\circ$; (b) $\vartheta_\alpha = 13.5^\circ$, $\vartheta_p = 12.7^\circ$; (c) $\vartheta_\alpha = 17.0^\circ$, $\vartheta_p = 18.3^\circ$; (d) $\vartheta_\alpha = 17.0^\circ$, $\vartheta_p = 35.0^\circ$. Continuous line—full calculation with the $M2$ model; dotted line—the same as the continuous line, but without 1S_0 np interaction; dot-dashed line—calculation done without Coulomb effects (for more details see the text). The dashed line is the phase-space factor in arbitrary units.

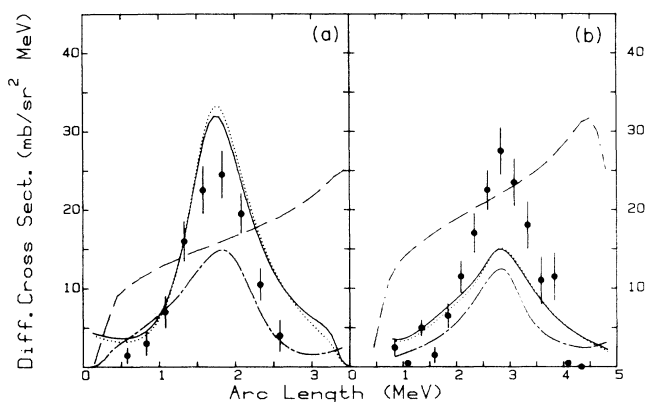


FIG. 2. Experimental data of the reaction $d + \alpha \rightarrow \alpha + p + n$ by the Köln group (Ref. 6). Kinematical configurations: (a) $E_d = 6$ MeV, $\vartheta_\alpha = 17.2^\circ$, $\vartheta_p = 42.0^\circ$; (b) $E_d = 7$ MeV; $\vartheta_\alpha = 21.3^\circ$, $\vartheta_p = 45.7^\circ$. Continuous line—full calculation with the $M2$ model; dotted line—calculation without 1S_0 interaction; dot-dashed line—Koike predictions. The dashed line is the phase-space factor in arbitrary units.

and without singlet np interaction, and a calculation as in Refs. 2, 6, 7, and 10 using model $M1$.

In Figs. 1 and 2 the continuous line is the full calculation within the model referred to as $M2$; the dotted line is the same type of calculation but without 1S_0 np interaction, and finally the dot-dashed line is a calculation without Coulomb effects in the Faddeev equations (the only Coulomb effect is the shift between the αn and αp resonances).

We now illustrate the various final state interaction (FSI) regions as they appear in Figs. 1 and 2. The kinematical configurations have been chosen in order to emphasize the role of the np FSI (Fig. 1) and of the αn FSI (Fig. 2). In Table I the values of the arc length corresponding to αn and np FSI's are listed.

In Fig. 1(a) the neutron-proton relative energy E_{np} is always smaller than 0.85 MeV and presents two minima at $s \approx 1.25$ MeV ($E_{np} \approx 0.27$ MeV) and at $s \approx 8$ MeV ($E_{np} \approx 0$); the relative energy between the alpha particle and the neutron ($E_{\alpha n}$) reaches the $^5\text{He}_{g.s.}$ resonance region ($E_{\alpha n} = 0.9$ MeV) at $s \approx 5$ and 8 MeV; the relative energy $E_{\alpha p}$ is smaller than 0.4 MeV for $s < 3$ MeV and $s > 9.5$ MeV and never reaches the value for the $^5\text{Li}_{g.s.}$ resonance. The cross sections are very small for $s < 3$ MeV and $s > 9$ MeV; this may be explained by the fact that the proton tends to be trapped by the Coulomb barrier of the α particle, thereby reducing the breakup amplitude. The peak at $s \approx 8$ MeV shows a constructive interference between αn and np FSI's; this can be seen both from the comparison of the dotted line to the continuous one and of the dot-dashed line to the experimental data. It should be noted that all the calculations (but not the experimental data), even without the inclusion of 1S_0 interaction, show a peak in the region of $s \approx 1$ MeV; this peak is not related to any specific dynamical mechanism such as the np FSI's, but is essentially due to the phase space factor¹⁵ (also plotted in the figure on an arbitrary scale). The $^5\text{He}_{g.s.}$ peak at $s \approx 5$ MeV is overestimated by all the calculations, but the con-

TABLE I. Arc length values for FSI regions.

Incident particle	Incident energy (MeV)	ϑ_α	ϑ_p	s (MeV)		s (MeV)	
				$(E_{\alpha n} \cong 0.9 \text{ MeV})$		$(E_{np} \cong 0)$	
α	11.3	12.7	13.5	4.9	8.1	1.25 ^a	8.0
α	11.3	13.5	12.7	3.9	7.3	1.20 ^b	7.5
α	11.3	17.0	18.3	2.3	4.4		4.4
α	11.3	17.0	35.0	1.0	4.7		0.9
d	6	17.2	42.0		1.85		
d	7	21.3	45.7		2.80		

^a $E_{np} \cong 0.27 \text{ MeV}$.

^b $E_{np} \cong 0.30 \text{ MeV}$.

tinuous line seems to reproduce the data better than the other calculations.

Figure 1(b) reflects the same behavior of Fig. 1(a); E_{np} also presents two minima at $s \cong 1.2 \text{ MeV}$ ($E_{np} \cong 0.3 \text{ MeV}$) and at $s \cong 7.5 \text{ MeV}$ ($E_{np} \cong 0$) and the same αn FSI's are present ($s \cong 3.9$ and 7.3 MeV).

In Fig. 1(c) E_{np} is always smaller than 0.3 MeV and there is only a relevant peak for $E_{np} \cong 0$ and $E_{\alpha n} = 0.9 \text{ MeV}$ at $s \cong 4.4 \text{ MeV}$, again indicating a constructive interference between these two FSI's.

As a general comment, in Figs. 1(a)–(c), where the kinematical configurations are nearly symmetric in angles, the continuous line qualitatively seems to reproduce the shape better than the other calculations; an overestimate of the singlet peak in the regions where $E_{np} \cong 0$ is present, as in Fig. 1 of Ref. 11.

In Fig. 1(d) a kinematical configuration where the two angles differ considerably is presented and the experimental data reflect a different behavior of the cross sections. The only relevant FSI seems to be the ${}^5\text{He}_{g.s.}$ FSI at $s \cong 4.7 \text{ MeV}$, whereas no experimental peak is present in the region $s \cong 0.9 \text{ MeV}$ where both np and αn FSI's contribute. The curve representing the calculation without Coulomb effects seems to reproduce the experimental behavior rather well. The peak of the continuous line originates from the singlet ($E_{np} = 0$).

From an experimental point of view, Coulomb-induced effects and in particular singlet np excitation seem to depend strongly on the kinematical configurations. In particular, the angle ϑ_{d^*} appears to be the relevant quantity; indeed when $\vartheta_{d^*} = 97^\circ$ [see Fig. 1(d)] the singlet interaction is not prominent, whereas when ϑ_{d^*} ranges from 33° to 47.5° [see, e.g., Figs. 1(a)–(c)] a distinct $E_{np} = 0$ peak emerges. This result confirms old measurements suggesting a large suppression of the d^* production around 90° .¹⁶ Phenomenologically this can be understood in terms of P -wave dominance of the α -nucleon interaction.¹⁷ On the other hand, the $M2$ calculations produce a rather isotropic distribution of d^* instead of giving an angular distribution like that of elastic scattering.

In Figs. 2(a) and (b) each peak corresponds to ${}^5\text{He}_{g.s.}$; the experimental data do not show any appreciable variation between Figs. 2(a) and (b). It has to be noted that ${}^3\text{Li}_{g.s.}$ excitation at $s \cong 3.8 \text{ MeV}$ in Fig. 2(b) is strongly

suppressed. The calculations of Koike¹⁰ consistently underestimate the ${}^5\text{He}_{g.s.}$ peak in both kinematical configurations, suggesting possible three-body effects not included in the Faddeev framework, in agreement with the fact that in the elastic scattering the 1^+ state of the intermediate ${}^6\text{Li}^*$ is described rather poorly.¹⁴ We would like to stress that also inclusive breakup measurements³ show that both Coulomb effects and the ${}^6\text{Li}^*$ 1^+ resonance are not yet adequately reproduced by numerical calculations of the type we have discussed at these low energies. It would therefore be interesting to investigate in detail from a theoretical point of view the elastic αd scattering in the ${}^6\text{Li}^*$ resonance region.

The importance of the difference of Coulomb effects between 6 and 7 MeV, as reflected in the continuous and dotted lines, is not clear and is possibly due to the inadequacy of the treatment of the Coulomb effects or of the approximation for the two-body interactions as suggested in Refs. 18 and 19.

In conclusion, the model calculations $M2$, although deficient in the detailed predictions as in Fig. 1(d) and Figs. 2, indicate that the size of the Coulomb effect can be important, even at not too small an energy as in Fig. 2(a); for the α -induced deuteron breakup it is particularly important to consider the Coulomb effects because they can induce np singlet FSI's. The singlet np FSI plays an important role, e.g., when it interferes constructively with αn FSI's as in Figs. 1(a)–(c). In conclusion, we would like to remark that a sensitivity to the 1S_0 interaction of the np FSI clearly appears both theoretically and experimentally. Whereas on general grounds the isospin breaking effects can be expected to be only a few percent, specifically in the $E_{np} = 0$ region there is a magnifying effect of the isospin breaking due to the 1S_0 FSI [see the peaks in Figs. 1(a)–(c) and in particular the comparison between the continuous and the dotted lines]. The dynamics of d^* production seems experimentally to be related to the dominance of the P -wave α -nucleon interaction.¹⁷ The model $M2$ on the other hand does not reproduce this result [see Fig. 1(d)]. A better theoretical calculation should account both for the angular distribution of the d^* production as well as for the suppression of the cross section for small values of the αp relative energy $E_{\alpha p}$ [see Fig. 1(a), $s < 3$ and $s > 9.5 \text{ MeV}$]. The last is a Coulomb effect which is complementary to the observed peak at maximum relative

energy of two charged particles in a three-body breakup.²⁰

As a final comment we would like to stress that since the $M2$ model is lacking in the detailed predictions of the d^* angular distribution, improvements in the α -nucleon interactions and in Coulomb corrections are needed for a better description of the α - d breakup.

The Bologna group would like to thank Mr. G. Busacchi for his skillful technical assistance and the staff members of the Laboratori Nazionali of Legnaro for hospitality and technical help. This work was supported in part by der Bundesministerium für Technologie (BMFT), Bonn, Federal Republic of Germany.

*Now at Bayer AG, Leverkusen, Federal Republic of Germany.

†Now at Ford AG, Köln, Federal Republic of Germany.

‡Present address: University of Notre Dame, South Bend, IN 46556.

¹T. Rausch, H. Zell, D. Wallenwein, and W. von Witsch, Nucl. Phys. **A222**, 429 (1974).

²M. Bruno, F. Cannata, M. D'Agostino, M. L. Fiandri, M. Frisoni, G. Vannini, and M. Lombardi, Nucl. Phys. **A386**, 269 (1982).

³R. C. Luhn, S. Sen, N. O. Gaiser, S. E. Darden, and Y. Koike, Phys. Rev. C **32**, 11 (1985); P. Doleschall, Nucl. Phys. **A407**, 29 (1983).

⁴M. Bruno, F. Cannata, M. D'Agostino, B. Jenny, W. Grüebler, V. König, P. A. Schmelzbach, and P. Doleschall, Nucl. Phys. **A407**, 29 (1983).

⁵I. Slaus, J. M. Lambert, P. A. Treado, F. D. Correll, R. E. Brown, R. A. Hardekopf, N. Jarmie, Y. Koike, and W. Grüebler, Nucl. Phys. **A397**, 205 (1983).

⁶H. Oswald, M. Buballa, J. Helten, M. Karus, B. Laumann, R. Melzer, P. Niessen, G. Rauprich, J. Schulte-Uebbing, and H. Paetz gen. Schieck, Nucl. Phys. **A435**, 77 (1985).

⁷H. Oswald, W. Burgmer, D. Gola, C. Heinrich, H. J. Helten, and H. Paetz gen. Schieck, Phys. Rev. Lett. **46**, 307 (1981).

⁸E. O. Alt, W. Sandhas, and H. J. Ziegelmann, Nucl. Phys. **A445**, 429 (1985).

⁹D. Gola and C. Heinrich, Nucl. Instrum. Methods **A243**, 424 (1986).

¹⁰Y. Koike, Nucl. Phys. **A301**, 411 (1978).

¹¹P. Doleschall, G. Bencze, M. Bruno, F. Cannata, and M. D'Agostino, Phys. Lett. **152B**, 1 (1985).

¹²J. M. Lambert, P. A. Treado, P. G. Roos, N. S. Chant, A. Nadasen, I. Slaus, and Y. Koike, Phys. Rev. C **26**, 357 (1982).

¹³Y. Koike, Prog. Theor. Phys. **59**, 87 (1978).

¹⁴M. Bruno, F. Cannata, M. D'Agostino, C. Maroni, I. Massa, and M. Lombardi, Nuovo Cimento **68A**, 35 (1982); L. S. Senhouse and T. A. Tombrello, Nucl. Phys. **57**, 624 (1964).

¹⁵G. G. Ohlsen, Nucl. Instrum. Methods **37**, 240 (1965).

¹⁶R. M. Vries, Ivo Slaus, Jules W. Sunier, T. A. Tombrello, and A. V. Nero, Phys. Rev. C **6**, 1447 (1972).

¹⁷C. Wertz and F. Cannata, Phys. Rev. C **24**, 394 (1981).

¹⁸C. Heinrich, Ph.D. dissertation, University of Hamburg, 1983 (unpublished).

¹⁹K. Hahn, Ph.D. dissertation, University of Tübingen, 1983 (unpublished).

²⁰H. Kröger, A. M. Machabe, and R. J. Slobodrian, Phys. Rev. C **32**, 628 (1985).